Ultrafast Plasmon Dynamics in Crystalline LiF Triggered by Intense Extreme UV Pulses

C. Fasolato,[1,*] F. Sacchetti,[1,2] P. Postorino,[3,2] P. Tozzi,[2] E. Principi,[4] A. Simoncig,[4] L. Foglia,[4] R. Mincigrucci,[4] F. Bencivenga,[4] C. Masciovecchio,[4] and C. Petrillo[1]

[1]*Università di Perugia, Dipartimento di Fisica e Geologia, I-06123 Perugia, Italy*
[2]*CNR Istituto Officina dei Materiali (IOM), I-06123 Perugia, Italy*
[3]*Università di Roma Sapienza, Dipartimento di Fisica, I-00100 Roma, Italy*
[4]*Elettra-Sincrotrone Trieste SCpA, I-34149 Basovizza, Trieste, Italy*

(Received 3 July 2019; revised manuscript received 12 February 2020; accepted 8 April 2020; published 7 May 2020)

An extreme ultraviolet pump and visible-light probe transmission experiment in crystalline LiF, carried out at the Free Electron Laser facility FERMI, revealed an oscillating time dependence of the plasmon mode excited in the high-density high-temperature electron plasma. The effect is interpreted as a fingerprint of the electron-ion interaction: the ion motion, shaped by the electron dynamic screening, induces, in turn, electron density fluctuations that cause the oscillation of the plasmon frequency at the timescale of the ion dynamics. Fitting the high resolution transmission data with an RPA model for the temperature-dependent dielectric function, which includes electron self-energy and electron-ion coupling, confirms the interpretation of the time modulation of the plasmon mode.

DOI: 10.1103/PhysRevLett.124.184801

Dense plasmas are a challenging subject and, despite more than a decade of intense experimental and theoretical investigations, they still represent a frontier in the knowledge of the electron system at arbitrary density and temperature, ranging from Fermi-degenerate liquid to strongly coupled plasma, to ideal electron gas regime. A comprehensive theory capable to connect different plasma regimes, to describe equilibrium properties and to model the system when brought out of equilibrium, is still lacking. Advances in experimental techniques make nowadays possible to carry out cutting edge experiments on electron plasmas in a wide range of thermodynamic conditions. Indeed, a variety of tailored methods and instruments are available, from inertial confinement fusion experiments [1] to short-pulse intense optical lasers for rapid heating to plasma conditions and fast probing [2], to free electron laser (FEL) sources which cover a wide spectral region from ultraviolet (UV) to x rays [3,4].

Within the pump and probe class of experiments, Thomson scattering is a solid and acknowledged technique for experimental investigation of dense plasmas at temperatures up to hundreds of eV, which enables one to measure the time evolution of the wave-vector and frequency-dependent response function of highly excited electrons, by visible-UV or x-ray probes [5]. Over a decade ago, spectrally resolved x-ray scattering experiments in dense plasmas were reported [6], providing measurements of the electron momentum distribution, temperature, and ionization state. The experimental potential brought in by FEL sources, which are characterized by tunability, focusing down to nanoscale, and the highly penetrating nature of ultrashort x-ray bursts, further prompted exploitation of Thomson scattering to explore collective excitations [7]. Pump and probe measurements on highly excited systems remain a major source of experimental data on dense plasmas and a reference for finite temperature time-dependent theories and computational approaches [8–10], even for the interacting electron gas model [10–13].

Here, we report on a pump and probe transmission experiment in crystalline LiF, pumped to high-temperature dense plasma conditions by the extreme UV (EUV) pulse of FERMI FEL [4] (Trieste, Italy), and probed by a delayed white visible pulse. Being transparent from infrared to ultraviolet, LiF is suitable for optical spectroscopy analysis. In the spectral region of visible light, plasmons can be detected for not too high electron number densities ($0.002 \leq n \leq 0.006$ Å^{-3}, corresponding to $6 \leq r_s \leq 8$). Plasmon measurements by x-ray Thomson scattering, despite the advantage of mapping the response function at finite momentum transfers [7,14], typically suffer of limited energy resolution. Indeed, the probe energy ($\sim$10 keV) exceeds that of the plasmon ($\sim$10 eV) by orders of magnitude, and the intense quasielastic peak can obscure the inelastic signal. Here, the plasmon peak is observed in the $q \to 0$ region by a visible probe, which greatly improves the energy resolution. Also, plasma conditions are attained differently from the standard, typically efficient, method of shock waves generated by high power optical laser heating. Indeed, the intense and short, EUV photon pulse available at FERMI [15] directly excites electrons in LiF from ground state to almost free, high-energy states characterized by very short lifetime ($\sim$1 fs) and rapid thermalization, because of strong electron-electron interactions [16,17]. With the electrons brought

to highly excited states, ions experience a modified lattice potential that is no more effective to keep them at the equilibrium positions. The crystal symmetry is lost and ions behave like a disordered system. With an initial RT velocity distribution, ions can cover rms distances of ~0.1 nm in ~100 fs. Energy transfer from electrons to ions proceeds through the much weaker electron-phonon interaction whose effects develop over longer timescales. Then, the picture, immediately after the FEL exciting pulse, is that of a high temperature electron plasma with a number density close to that of solid LiF, and charge neutralized by a disordered positive ion background. The described mechanism is quite different from the laser excitation through shock waves, where both the initial energy transfer from the pump and the following energy redistribution among the system's different degrees of freedom involve evenly electrons and ions.

Our optical transmission experiment at FERMI provides evidence for the plasmon mode in dense electron gas produced in insulating LiF and shows that the subpicosecond time evolution of this mode is characterized by an oscillating behavior, a rather unexpected and novel experimental result. To analyze and interpret the oscillating feature, a model for the response function based on the RPA dielectric function, properly modified to account for electron-electron and electron-phonon interactions, is applied.

The experiment was carried out at the EIS-TIMEX beam line [18], where an almost jitter free (~10 fs) pump-probe measurement is possible thanks to the seeded nature of the FEL lasing process [15]. The high-quality LiF single crystal was 1 mm thick, 10×10 mm^2 wide, with (100) surface. 15 μJ/pulse energy were released on LiF by EUV photons of FEL pump pulse ($E = 33.38$ eV, $\lambda = 37.14$ nm, pulse length ~80 fs, spot size at the sample ~30 μm). The generated plasma was probed by a supercontinuum pulse in the visible region ($450 \leq \lambda \leq 750$ nm), produced by the FEL seed laser for users, with a very good temporal resolution achieved by controlled chirping. The pump-probe coincidence time $t_0(\lambda)$ was determined experimentally by monitoring the optical response of a reference sample. Experimental details, including a schematics of the setup, are reported in the Supplemental Material (SM) [19]. The transmitted spectrum was collected at each FEL pulse, first without, then with, the pump impinging on a pristine point of the sample only once. The effects of sample damage were determined by collecting, each time, an additional transmission spectrum a few milliseconds after the pump pulse and data were consistently corrected for. Transmission was measured at variable delay, over a $\lesssim 2$ ps range from negative to positive delay times at 100 fs time steps. Various sets of same collected data were averaged to minimize the pump and the probe intensity fluctuations.

Accounting for sample damage, the transmission was expressed as $T_{\mathrm{eff}}(\lambda, t) = I(\lambda, t)/\{[1 - \theta(t - t_0)]I_0(\lambda) + \theta(t - t_0)I_\infty(\lambda)\}$, $\theta(t)$ the step function, t_0 the pump-probe coincidence time measured as a function of λ, $I(\lambda, t)$, $I_0(\lambda)$, and $I_\infty(\lambda)$ the transmitted intensities with pump-on and delay t, pump-off, and a few milliseconds after pump arrival, respectively. Reduction of the measured pump-on intensities due to reflectivity, as observed in very high-density plasmas [20], additional to absorption, was neglected as of minor impact in this experiment. Indeed, the reflectivity ranges from 4% up to 18% almost linearly with increasing wavelength (see SM [19]). Figure 1 shows $I(\lambda, t = 1.3\ \mathrm{ps})$, $I_0(\lambda)$, and $I_\infty(\lambda)$, while $T_{\mathrm{eff}}(\lambda, t)$ at four selected λ values is plotted in Fig. 2. For $t < t_0$, the transmission is consistently close to one as the averaging procedure correctly cancels out the effects of probe intensity fluctuations. For $t > t_0$ a sudden transmission drop occurs within 100 fs around t_0, corresponding to a very fast dynamics of the system, which cannot be ascribed

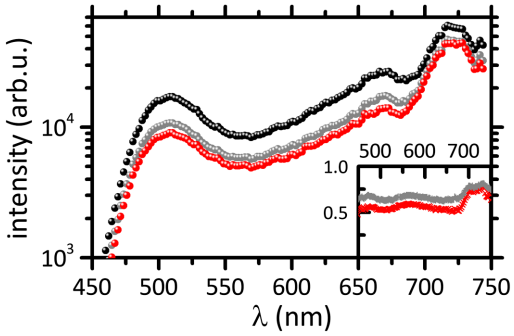

FIG. 1. Transmitted intensity $I(\lambda, t)$ versus λ at $t = 1.3$ ps (red dots); $I_0(\lambda)$ collected 1 ps before pump (black dots); $I_\infty(\lambda)$ collected some milliseconds after the pump (gray dots). The inset shows the ratios $I(\lambda, t = 1.3\ \mathrm{ps})/I_0(\lambda)$ (red crosses) and $I_\infty(\lambda)/I_0(\lambda)$ (gray crosses).

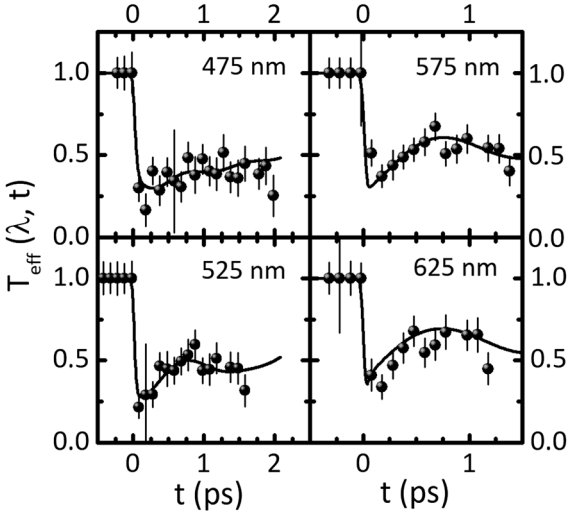

FIG. 2. Sample transmission $T_{\mathrm{eff}}(\lambda, t)$ versus pump-probe delay time, at four selected wavelengths. The coincidence time t_0 is set to zero. Continuous lines are the best-fit curves to the data according to Eq. (2).

to the electron-ion interactions, followed by a slower time evolution over a 1–2 ps window.

To describe the complexity of the behavior observed in the excited plasma, specifically the oscillation in the time dependence of the plasma transmission, a proper theoretical model of the dielectric function is necessary. Indeed, we can write $T(\lambda,t)=\exp[-\mu(\lambda,t)d]$, d being the unknown plasma thickness, $\mu(\lambda,t)=n(t)\sigma(\lambda,t)$ the wavelength- and time-dependent linear absorption coefficient with $\sigma(\lambda,t)$ the absorption cross section proportional to the imaginary part of the inverse dielectric function and $n(t)$ the time-dependent electron number density. $n(t)$ can be modeled by a function abruptly increasing during pumping, followed by a slow exponential decrease, that is $n(t)=n_0/2\exp(-\gamma t)\{1+\tanh[t/\tau_0]\}$, where γ is an electron density decay constant and τ_0 is a time width describing the fast increase of electron density upon arrival of the pump pulse [14]. As transmission was measured in the visible frequency range, data are confined to the very low q region. The dielectric function $\epsilon(q,\omega)$ is based on RPA at $T>0$, as better detailed in the SM [19]. In the long wavelength limit $q\to 0$ and $\omega\gg qk_F$ (Rydberg units throughout the text), it reads

$$\epsilon(0,\omega)=1-\frac{8e^2}{\pi\omega^2}\int_0^\infty dk k^2[1+i2C_{k_F}(k^2-\epsilon_F)f(k^2)], \tag{1}$$

with $f(k^2)$ the Fermi distribution function calculated using the chemical potential $\mu(T_e)$ at the electron temperature T_e. Finite damping of the electron states, caused by electron-electron interactions, is accounted for by approximating the single particle energy $\epsilon_{\mathbf{k}}$ as $\epsilon_{\mathbf{k}}+iC_{k_F}(\epsilon_{\mathbf{k}}-\epsilon_F)^2$, where the imaginary part is the electron self-energy contribution [21] at $T=0$ and $\epsilon_{\mathbf{k}}$ close to the Fermi energy ϵ_F. Although more complex and T_e-dependent corrections might be considered [16,22], this simple approximation for the self-energy including one electron states lifetime, provides a model adequate to analyze the transmission data. In Eq. (1), the imaginary part is determined along the quasiparticle dispersion relation $\epsilon_{\mathbf{k}}=k^2$ as suggested in Ref. [23]. With C_{k_F} provided by Hedin's approximation [16,24], the dielectric function can be numerically calculated and the poles of the response function $\Im[1/\epsilon(0,\omega)]$ obtained. The imaginary part of $\epsilon(0,\omega)$ is temperature dependent and density dependent, which enables evaluating the electron temperature T_e from the imaginary part once the electron density n is obtained from the T_e-independent real part of $\epsilon(0,\omega)$. The model is applied under the assumption $T_e\gg T_i$, with T_i the temperature of the ion background, as the transfer of energy from electrons to ions is not expected to be the dominant interaction mechanism at delay times shorter than 2 ps. Indeed, thermalization of ion degrees of freedom occurs through two major mechanisms: direct interaction of phononlike modes with electrons and single particle electron-ion collisions [25,26], with thermalization times 3.2 and 2.6 ps, respectively (see SM [19]).

The experimental time-dependent transmission data were fitted using the model dielectric function of Eq. (1), redrawn in a computationally more manageable form (see SM [19]), with

$$\mu(\lambda,t)d=\alpha n(t)\left\{\frac{[\Gamma_r\lambda_p(t)\lambda]^2}{[\lambda^2-\lambda_p^2(t)]^2+(\Gamma_r\lambda)^4}\right\} \tag{2}$$

$\lambda_p(t)=2\pi c/\omega_p(t)$, ω_p plasma frequency and Γ_r resonance width. The sample thickness d, not obtained by independent measurements, is contained in the proportionality constant α that incorporates the effects of systematic errors.

The time-dependent oscillation clearly observed in $T_{\mathrm{eff}}(\lambda,t)$ in Fig. 2 needs to be modeled. The simplest approach was to introduce in Eq. (2) a time dependence for the plasmon wavelength reproducing the observed oscillation at low frequency, that is $\lambda_p(t)=\{\beta_0+\beta_1\cos[\Omega_{\mathrm{ion}}(t-t_1)]\}/\sqrt{n(t)}$, where $\beta_0=\sqrt{\pi mc}/e$, Ω_{ion} a slow oscillation frequency that can sensibly be attributed to the ion plasma, and β_1 a coupling coefficient between electron and ion plasmas. The time t_1 measures the phase shift between electron and ion oscillations. Indeed, a consistent analysis of the experimental results requires accounting for the coupled dynamics of electrons and ions, under the assumption of system neutrality. Assuming a phononlike nature for the low frequency oscillation, the coupled dynamics of a system of ions embedded within a high-temperature electron plasma can be described using the simplified analysis of collective modes in liquid metals [27]. Ion density fluctuations are described by the position fluctuation operator $Q_{\mathbf{q}}(t)$, which is a solution of motion equation $\ddot{Q}_{\mathbf{q}}(t)+\Omega_{ip}^2Q_{\mathbf{q}}(t)+v_{\mathbf{q}}\rho_{\mathbf{q}}(t)=0$, $v_{\mathbf{q}}$ the electron-ion interaction, $\Omega_{ip}^2=4\pi(Ze)^2n_{\mathrm{ion}}/M_{\mathrm{ion}}$ the classical ion plasma frequency, squared, and $\rho_{\mathbf{q}}(t)$ the electron density fluctuation induced by the ion motion. Z, n_{ion}, and M_{ion} are ion charge, density, and mass, respectively. For a two-component ion system, like LiF [28,29], the ion plasma frequency Ω_{ip} can be written as $\Omega_{ip}^2=4\pi e^2[Z_1^2n_1/M_1+Z_2^2n_2/M_2]$. The ion collective mode dispersion relation, obtained solving the motion equation, is cast in the form

$$\Omega_{\mathrm{ion}}^2(q,T_e)=\Omega_{ip}^2\left[1-U+\frac{1}{\epsilon(q,\Omega_{\mathrm{ion}}(q,T_e);T_e)}\right], \tag{3}$$

where the dielectric function at temperature T_e, $\epsilon[q,\Omega_{\mathrm{ion}}(q,T_e);T_e]$ is calculated self-consistently, $U=n/n_{\mathrm{ion}}$ is a constant related to charge unbalance. For a charged plasma perfectly charge neutralized, $U=1$ and the long wavelength limit of Eq. (3), at $T_e=0$, returns the well-known Bohm-Staver relationship for the longitudinal collective mode frequency, $\Omega_{\mathrm{ion}}^{\mathrm{BS}}(q)=\Omega_{ip}q/k_s$ that goes to

0 for $q \to 0$, with k_s the Thomas-Fermi wave vector embodying the electron gas screening length. When $n = n_{\mathrm{ion}}$, the ion plasma oscillation assumes the characteristics of an acoustic mode [27,30,31]. In the present pump and probe experiment in LiF, charge compensation cannot be assumed *a priori* and, consequently, U was not fixed equal to 1.

Equation (2), coupled to the ansatz for the electron plasma wavelength $\lambda_p(t)$, provides a comprehensive fitting model to the experimental data, as detailed in SM [19]. Here, we recall that the global fit was applied to all the 502 time- and wavelength-dependent data, it resulted accurate and stable with a reduced $\chi^2 = 1.20$. The best-fit parameters reported in Table I of SM [19] support an overall coherent picture of the process in LiF. The electron density $n(t)$ is characterized by $n_0 = (0.399 \pm 0.071) \times 10^{22}\, e/\mathrm{cm}^3$, a decay parameter $\gamma \sim 0$ suggests the electron plasma is fairly stable over the sampling time, and $\tau_0 = 54 \pm 20$ fs confirms plasma generation during the short pump pulse. Then, within the explored time interval ($t > t_0$), the density remains almost constant while the temperature, obtained from $\Im[1/\epsilon(0,\omega)]$, decreases with time remaining in the 10^5 K range as a consequence of the interaction with ions. The density n_0, although smaller than n_{mol} of solid LiF ($n_{\mathrm{mol}} = 6.23 \times 10^{22}$ mol/cm^3), is still fairly high for the plasma to be placed at the boundary of the strongly coupled plasma with the ideal plasma region, being $T_e \sim 10^5$ K. Density and temperature here obtained can be safely ascribed to the electron plasma, since in the considered time range the ion dynamics contributes to definitely a much lower extent. A further important indication comes from the $t = 0$ value of $\Gamma_r = 0.65 \pm 0.04$ that indicates the strong damping of the electron plasma, as expected at high temperature and relatively high-density conditions. The ion plasma oscillation frequency resulted $\Omega_{\mathrm{ion}} = 3.2 \pm 1.0\,\mathrm{ps}^{-1}$, which might suggest an optical-like character for the collective mode. However, optical phonon modes in crystalline LiF [32] have frequencies much higher than Ω_{ion}, which rules out this interpretation. The best-fit value of Ω_{ion} can be used in Eq. (3) to estimate the charge density unbalance parameter U. We found $U = 0.99$ that is a result very close to the ideal value corresponding to perfect neutrality of the system.

The best-fitting curves for $T_{\mathrm{eff}}(\lambda, t)$ are compared with the experimental data in Fig. 2, while a $3d$ mapping is shown in Fig. 3. Oscillation with time is quite apparent over the region 0–1 ps. The time dependence of the plasmon resonance wavelength $\lambda_p(t)$ is shown in Fig. 4(a), where a well-resolved oscillation takes place around the average resonance wavelength $\lambda_0 = \beta_0/\sqrt{n(t)} = \beta_0/\sqrt{n_0}$ when $t > \tau_0$. Using λ_0 resulting from the time average of $\lambda_p(t)$, it is possible to obtain the electron density n_0 that, vice versa, if taken from Table I in SM [19] as one of the best-fit parameters, can be used to deduce a value for λ_0. Results from the two procedures were highly consistent

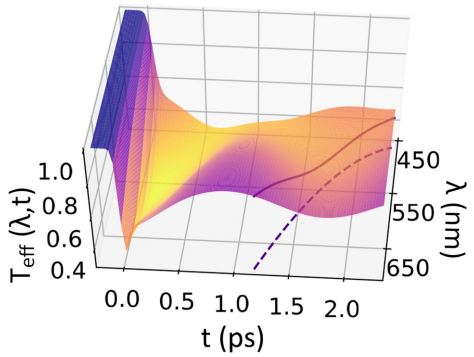

FIG. 3. $3d$ mapping of $T_{\mathrm{eff}}(\lambda, t)$ obtained from the fitting model to Eq. (2). The dashed line in the (λ, t) plane is the region accessible to the experiment. The continuous line is the transmission curve calculated along the border of the accessible region.

with λ_0 taking the value 528 ± 47 nm. In Fig. 4(b), $\Im[1/\epsilon(0,\omega)]$ directly calculated from Eq. (1) is plotted versus λ at $t = 1$ ps in comparison with the data shown as $[\mu(\lambda, t)d]/[\alpha n(t)]$. This figure shows the quality of the fit in comparison with the theoretical model of the resonance curve.

The energy released by the pump pulse (33.4 eV), which would correspond to ~20 nm mean free path in solid LiF, is high enough to cause a rapid electronic excitation. As the FEL pulse delivers about 2.8×10^{12} photons, each one exciting ~1.5 electrons to thermal energy, ideally $\sim 4.2 \times 10^{12}$ electrons per pulse are brought to an excited state. The exact volume of the generated plasma cannot be easily determined, but the observation of the damaged region suggests it as a cylinder ~15 μm radius and 2 μm thickness, that is big enough to describe the electron gas as homogeneous. These estimates for plasma volume and number of excited electrons return $\sim 0.29 \times 10^{22}\ e/\mathrm{cm}^3$ for the electron density, which is consistent with the experiment. In SM [19] we also introduce an empiric model for plasma production in EUV regime which describes the density dependence on plasma evolution, i.e., on propagating damage.

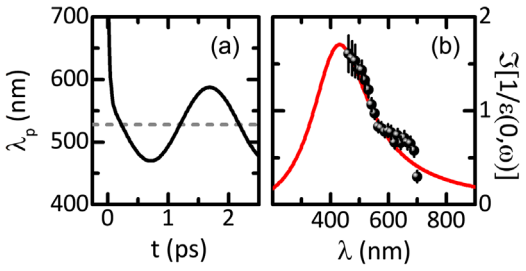

FIG. 4. (a) Time dependence of the plasmon wavelength $\lambda_p(t)$ after the fitting model. Horizontal dashed line: the average value λ_0. (b) Experimental resonance line (dots) in comparison with the model inverse dielectric function $\Im[1/\epsilon(0,\omega)]$ calculated at $T_e = 10^5$ K, $r_s = 7.4$, and $t = 1$ ps.

In summary, a high-temperature, high-density electron plasma in LiF was produced by the EUV FEL pumping. Transmission measurements by visible-light probe, as characterized by high resolution, namely 10 meV, enabled direct determination of the plasmon resonance width. Accurate information on electron density and temperature was obtained from the plasmon features ($k_B T_e \simeq 8.4$ eV from the line shape). Notably, we observed a time dependence of the electron plasma resonance, which is evidence for the coupled ion-electron plasma dynamics. Indeed, the proposed analysis supports the interpretation of the observed time oscillation as a feature of electron density fluctuations driven by partial electron screening of the ionic plasma oscillations and revealed at the frequencies of the ion motion. The time dependence of the electron plasma frequency is a fingerprint of the electron-ion interaction that, to our knowledge, is observed here for the first time as an ion induced effect on the collective electron density fluctuation mode. It is worth mentioning that the findings of this experiment show some similarity with another experiment recently carried out at EIS-TIMEX beam line on NiO sample [33]. In that case, sample exposure to an intense FEL pump was found to trigger a magnon of 0.86 THz frequency. An oscillation over a similar frequency region was also observed as a result of the IR 50 PW/cm^2 laser pumping of borosilicate glass [34]. It is then important to understand the time response of plasma generated through very different mechanisms. Typically, the effects of electron-phonon coupling are described by the screened interaction and are observed through the renormalization of the phonon dispersion curves or directly through the dissipative processes in the electron dynamics. The present result emphasizes the screening effects on the electron plasma mode. This is a novel observation that deserves further intense investigation by companion experiments using both high and low energy pumps on diverse samples to draw a consistent picture of the electron-phonon interaction effects in dense plasmas.

*Corresponding author.
claudia.fasolato@unipg.it

[1] O. A. Hurricane, D. A. Callahan, D. T. Casey *et al.*, Nature (London) **506**, 343 (2014).
[2] L. B. Fletcher, H. J. Lee *et al.*, Nat. Photonics **9**, 274 (2015).
[3] C. Bostedt, S. Boutet, D. M. Fritz, Z. Huang, H. J. Lee, H. T. Lemke, A. Robert, W. F. Schlotter, J. J. Turner, and G. J. Williams, Rev. Mod. Phys. **88**, 015007 (2016).
[4] E. Allaria, R. Appio *et al.*, Nat. Photonics **6**, 699 (2012).
[5] S. H. Glenzer and R. Redmer, Rev. Mod. Phys. **81**, 1625 (2009).
[6] S. H. Glenzer, G. Gregori, R. W. Lee, F. J. Rogers, S. W. Pollaine, and O. L. Landen, Phys. Rev. Lett. **90**, 175002 (2003).
[7] S. H. Glenzer, O. L. Landen *et al.*, Phys. Rev. Lett. **98**, 065002 (2007).
[8] E. Runge and E. K. U. Gross, Phys. Rev. Lett. **52**, 997 (1984).
[9] *Frontiers and Challenges in Warm Dense Matter*, edited by F. Graziani, M. Desjarlais, R. Redmer, and S. B. Trickey (Springer, New York, 2014).
[10] S. Groth, T. Schoof, T. Dornheim, and M. Bonitz, Phys. Rev. B **93**, 085102 (2016).
[11] E. W. Brown, B. K. Clark, J. L. DuBois, and D. M. Ceperley, Phys. Rev. Lett. **110**, 146405 (2013).
[12] T. Schoof, S. Groth, J. Vorberger, and M. Bonitz, Phys. Rev. Lett. **115**, 130402 (2015).
[13] C. Fasolato, F. Sacchetti, P. Tozzi, and C. Petrillo, Solid State Commun. **260**, 30 (2017).
[14] R. Thiele, T. Bornath, C. Fortmann, A. Höll, R. Redmer, H. Reinholz, G. Röpke, A. Wierling, S. H. Glenzer, and G. Gregori, Phys. Rev. E **78**, 026411 (2008).
[15] M. B. Danailov, F. Bencivenga *et al.*, Opt. Express **22**, 12869 (2014).
[16] L. Hedin, Phys. Rev. **139**, A796 (1965).
[17] C. Fortmann, Phys. Rev. E **79**, 016404 (2009).
[18] C. Masciovecchio, A. Battistoni *et al.*, J. Synchrotron Radiat. **22**, 553 (2015).
[19] See Supplemental Material at http://link.aps.org/supplemental/10.1103/PhysRevLett.124.184801 for details on the model response function and data fitting, ion thermalization and plasma production processes, and on the experimental setup.
[20] L. Chopineau, A. Leblanc, G. Blaclard, A. Denoeud, M. Thévenet, J.-L. Vay, G. Bonnaud, P. Martin, H. Vincenti, and F. Quéré, Phys. Rev. X, **9** 011050 (2019).
[21] J. M. Luttinger and J. C. Ward, Phys. Rev. **118**, 1417 (1960).
[22] A. L. Kutepov and G. Kotliar, Phys. Rev. B **96**, 035108 (2017).
[23] L. J. Sham and W. Kohn, Phys. Rev. **145**, 561 (1966).
[24] C. Petrillo and F. Sacchetti, Phys. Rev. B **38**, 3834 (1988).
[25] M. Dawson, Phys. Fluids **7**, 981 (1964).
[26] A. Richardson, *2019 NRL Plasma Formulary*, https://www.nrl.navy.mil/ppd/sites/www.nrl.navy.mil.ppd/files/pdfs/NRL_Formulary_2019.pdf.
[27] L. Sani, C. Petrillo, and F. Sacchetti, Phys. Rev. B **90**, 024207 (2014).
[28] D. Pines and P. Nozieres, *The Theory of Quantum Liquids* (Benjamin, New York, 1966), Vol. I; D. Pines, *Elementary Excitations in Solids* (Benjamin, New York, 1963).
[29] L. E. Bove, F. Sacchetti, C. Petrillo, and B. Dorner, Phys. Rev. Lett. **85**, 5352 (2000).
[30] L. E. Bove, F. Sacchetti, C. Petrillo, B. Dorner, F. Formisano, and F. Barocchi, Phys. Rev. Lett. **87**, 215504 (2001).
[31] L. E. Bove, B. Dorner, C. Petrillo, F. Sacchetti, and J.-B. Suck, Phys. Rev. B **68**, 024208 (2003).
[32] G. Dolling, H. G. Smith, R. M. Nicklow, P. R. Vijayaraghavan, and M. K. Wilkinson, Phys. Rev. **168**, 970 (1968).
[33] A. Simoncig, R. Mincigrucci *et al.*, Phys. Rev. Mater. **1**, 073802 (2017).
[34] A. Adak, A. P. L. Robinson, P. K. Singh, G. Chatterjee, A. D. Lad, J. Pasley, and G. R. Kumar, Phys. Rev. Lett. **114**, 115001 (2015).